AAPM REPORT NO. 96

The Measurement, Reporting, and Management of Radiation Dose in CT

Report of AAPM Task Group 23

of the Diagnostic Imaging Council CT Committee

January 2008

NOTE: The previously published version had incorrect values in Table 3, page 13, for the "k" factor in the first 2 rows of the "1-year-old" column. This was corrected effective April 3, 2008.

ISBN: 978-1-888340-73-0
ISSN: 0271-7344

Published by
American Association of Physicists in Medicine
One Physics Ellipse
College Park, MD 20740-3846

AAPM REPORT NO. 96

The Measurement, Reporting, and Management of Radiation Dose in CT

Report of AAPM Task Group 23: CT Dosimetry

Diagnostic Imaging Council CT Committee

Task Group Members:

Cynthia McCollough, Chairperson
Dianna Cody
Sue Edyvean
Rich Geise
Bob Gould
Nicholas Keat
Walter Huda
Phil Judy
Willi Kalender
Mike McNitt-Gray
Rick Morin
Tom Payne
Stanley Stern
Larry Rothenberg
Paul Shrimpton, Consultant
Jan Timmer, Consultant
Charles Wilson, Consultant

This page intentionally left blank.

CONTENTS

This page intentionally left blank.

1. INTRODUCTION

Since the introduction of helical computed tomography (CT) in the early 1990s, the technology and capabilities of CT scanners have changed tremendously (helical and spiral CT are equivalent technologies; for consistency, the term "helical" will be used throughout). The introduction of dual-slice systems in 1994 and multislice systems in 1998 (four detector arrays along the z-axis) has further accelerated the implementation of many new clinical applications[1–3]. The number of slices, or data channels, acquired per axial rotation has increased, with 16- and 64-slice systems now available (as well as models having 2, 6, 8, 10, 32, and 40 slices). Soon even larger detector arrays and axial coverage per rotation (>4 cm) will be commercially available, with results from a 256-slice scanner having already been published[4]. These tremendous strides in technology have resulted in many changes in the clinical use of CT. These include, but are not limited to, increased use of multiphase exams, vascular and cardiac exams, perfusion imaging, and screening exams (primarily the heart, chest, and colon, but also self-referred "whole-body"screening exams). Each of these applications prompts the need for discussion of radiation risk versus medical benefit. In addition, the public press in the United States, following publication by the *American Journal of Roentgenology* of two articles[5,6] on risks to pediatric patients from CT, has begun to scrutinize radiation dose levels from all CT examinations. Subsequent reports in the popular media have increased the concern of patients and parents of pediatric patients undergoing medically appropriate CT examinations[7].

The importance of radiation dose from x-ray CT has been underscored recently by the attention given in the scientific literature to issues of dose and the associated risk[5,6,8–13]. The dose levels imparted in CT exceed those from conventional radiography and fluoroscopy and the use of CT continues to grow, often by 10% to 15% per year[14,15]. According to 2006 data, approximately 62 million CT examinations were performed in hospitals and outpatient imaging facilities in the United States[16]. Thus, CT will continue to contribute a significant portion of the total collective dose delivered to the public from medical procedures involving ionizing radiation[14,15].

The rapid evolution of CT technology and the resultant explosion in new clinical applications, including cardiac CT, combined with the significance of CT dose levels, have created a compelling need to teach, understand, and use detailed information regarding CT dose.

All of these factors have created a need for the AAPM to provide professional, expert guidance regarding matters related to CT dose. Fundamental definitions of CT dose parameters require review and, perhaps reinterpretation, as CT technology evolves: some parameter definitions are not being used consistently, some are out of date, and some are more relevant than others with respect to patient risk or newer scanner designs. Hence, this task group, consisting of experts in the field of x-ray CT, was formed to address the following:

1. Provide guidance from the AAPM to the International Electrotechnical Commission (IEC) and U.S. Food and Drug Administration (FDA) and facilitate international consensus regarding:
   a. CT dose parameter definitions.
   b. CT dose measurements.
   c. Appropriate use of CT dose and risk parameters

2. Educate AAPM members regarding:
   a. CT dose definitions and measurements.
   b. European Guidelines on Quality Criteria for Computed Tomography, and other relevant international publications.
   c. Reasonable dose levels for routine CT examinations.

2. OVERVIEW OF MULTIPLE-DETECTOR-ROW CT (MDCT) TECHNOLOGY

The "multiple-detector-row" nature of MDCT scanners refers to the use of multiple detector arrays (rows) along the z-direction (perpendicular to the axial CT plane). Currently available MDCT scanners utilize third-generation CT geometry in which an arc of detectors and the x-ray tube(s) rotate together. All MDCT scanners use a slip-ring gantry, allowing helical acquisition at rotation speeds as fast as 0.33 seconds for a full rotation of the x-ray tube about the isocenter[17,18].

These scanners offer tremendous flexibility because of their advances not just in detector technology, but also in data acquisition systems (DAS), x-ray tube design and other subsystems. One illustration of this is that while MDCT scanners have multiple rows of detectors, the data collected from multiple rows can be combined as though they were collected from one detector. To describe this behavior, the term "channel" has been used, where a channel is the smallest unit in the z-direction from which data are independently collected. Therefore, if data from multiple detector rows are collected in such a way that those individual rows are combined (and the ability to determine from which row the data was originally collected is lost), then these rows form a channel.

Currently, commercial MDCT systems are capable of acquiring up to 64 channels of data (along the z-direction) simultaneously. Other values for N_{max}, the maximum number of independent channels acquired along the z-axis, for current commercially available MDCT systems include: 2, 4, 6, 8, 10, 16, 32, and 40. For axial data acquisitions, each channel collects sufficient data to create one "slice" or image, so as many as N_{max} independent images along the z-axis could theoretically be reconstructed. For narrow slice widths, however, cone-beam geometrical considerations may limit the number of allowed images per rotation to less than N_{max}. For example, one manufacturer's 16-slice scanner allows sixteen 1.5-mm channels for helical acquisitions, but only twelve 1.5-mm channels for sequential acquisitions because of cone-beam considerations. Alternatively, the data from multiple channels can be added together to create fewer than N_{max} images per gantry rotation, each image having a relatively wider width. Compared to single-detector-row CT (SDCT), MDCT systems allow faster acquisitions of a volume of data with less heat load on the x-ray tube (both by a factor of up to N_{max}). Sixty-four-channel systems appeared on the market in the middle of 2004, sixteen-channel scanner models were announced at the end of 2001, and four-channel systems were introduced in late 1998. A 256-channel system is anticipated in 2008.

Figure 1 illustrates the difference between an SDCT scanner and an MDCT scanner from the same vendor. The fundamental difference is the use of multiple detector-rows along the z-direction. In SDCT, the slice width is primarily determined by the pre-patient x-ray collimation (post-patient collimation was used on some SDCT scanners models). In MDCT, the z-extent of the data acquisition is determined by the pre-patient x-ray beam collimation, but the slice width of the image(s) is primarily defined by the detector configuration (the way in which detector elements are combined into data channels along the z-axis). Throughout this report, the total width of the pre-patient collimation will be referred to as the "beam collimation."

Figure 2 illustrates different detector configurations (along the z-direction) used by MDCT vendors for their 4-channel systems. While the GE detector comprises 16 identically sized detector rows, the Siemens, Philips (previously Marconi), and Toshiba systems utilize variably sized detector-rows along the z-direction. With the variable detector-size design, the beam collimation and detector configuration can be chosen in such a manner as to obtain *effective* detector widths other than those of the detector rows *per se*. For example, the 4-channel Siemens and Philips systems are capable of acquiring four 1-mm slices (i.e., 4×1 mm detector configuration) by set-

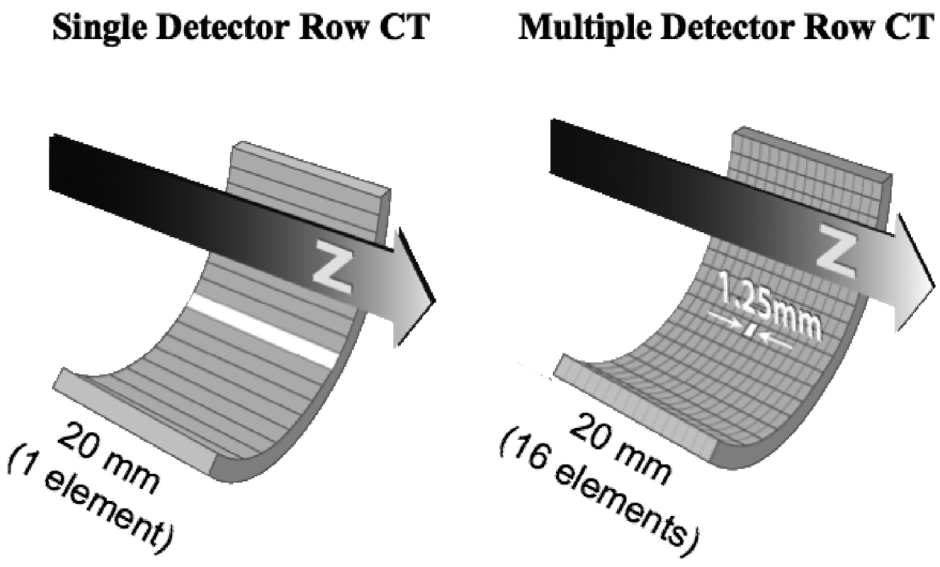

Figure 1. The single-detector row CT (SDCT) system on the left has one detector element along the longitudinal axis and many (approx. 900) elements on the arc around the patient. The width of the detector (relative to the center of the gantry) is 20 mm, although the maximum beam width is only 10 mm. Thus the detector is wider than the x-ray beam. The multiple-detector-row CT (MDCT) system on the right has 16 1.25-mm detector elements along the longitudinal axis for EACH of the approximately 900 positions around the patient. The width of the detector is also 20 mm at isocenter. The four data channels allow the acquisition of four simultaneous slices, of either 1.25, 2.5, 3.75, or 5 mm width.

ting the beam collimation to 4 mm. (Throughout this report, the detector configuration will be represented by the product of the number of independent data channels N and the width, along the z-direction at isocenter, imaged by one detector channel T, or $N \times T$ mm). This 4×1-mm mode fully irradiates the two central 1-mm detector elements and partially irradiates the two neighboring 1.5-mm rows to effectively give a 4×1 mm acquisition. This is accomplished with use of post-patient collimation along the z-axis. Figure 3 details the MDCT detector geometries for 64- channel systems from four major manufacturers.

As noted above, MDCT allows information from multiple detector rows to be combined into one data channel. For example, when the 4-channel Toshiba system utilizes its maximum beam collimation (32 mm), four 8-mm virtual detector rows may be formed by combining the signal from eight 1-mm wide detector-rows into a single channel. A significant advantage of MDCT is that signals from multiple data channels may be summed to yield slice widths that are larger than the width corresponding to a given data channel. This may be done retrospectively, allowing, for example, a 4×1.25-mm data acquisition to be presented as one 5-mm thick slice, two 2.5-mm slices, four 1.25-mm slices, or all of these options.

When specifying an imaging protocol, it is very important to note the detector configuration used to acquire the desired slice thickness, as this significantly affects the subsequent retrospective reconstruction options (for thinner or thicker images) and the radiation efficiency of the system (i.e., patient dose). For instance, using an MDCT scanner one might acquire 5-mm slices either by using a wide beam collimation (4×5 mm) or by utilizing a narrow beam collimation (4×1.25 mm). The wide beam collimation allows much faster z-coverage, while the slower narrow beam

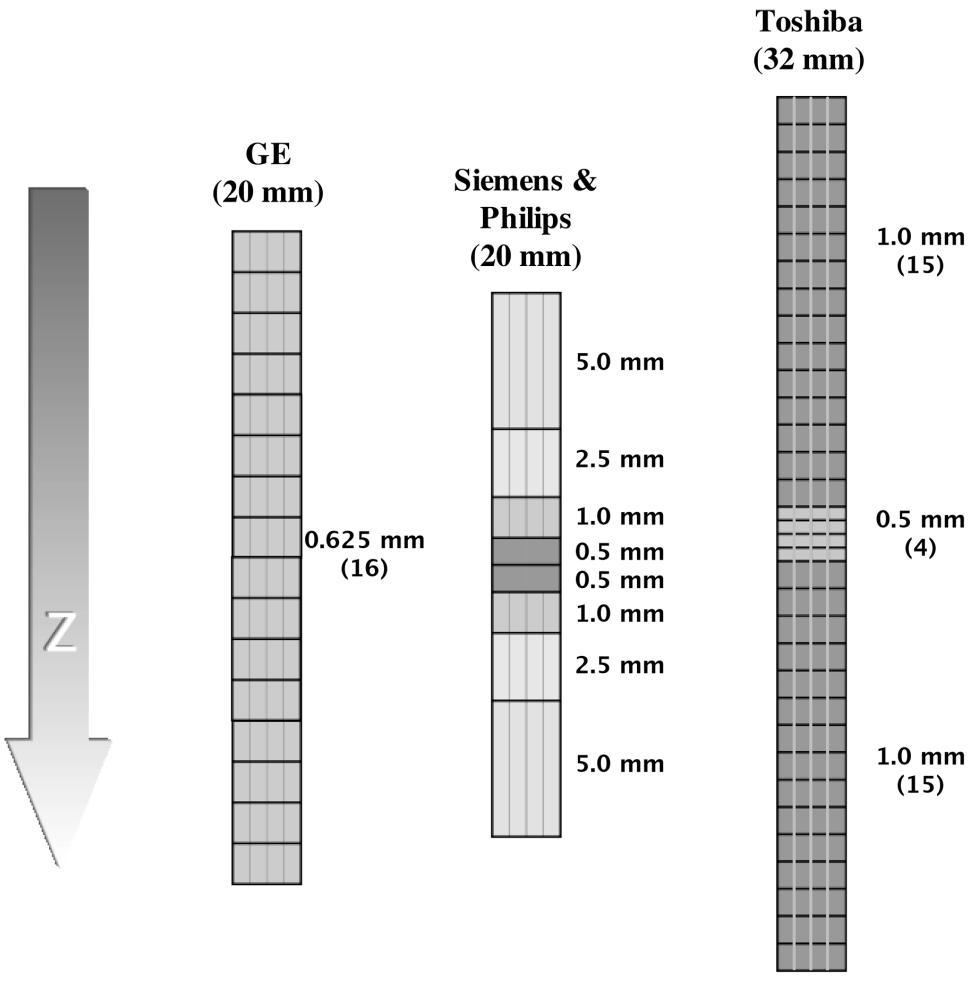

Figure 2. Diagram of the detector geometries used in the 4-channel MDCT systems from the four major CT manufacturers. The detector geometry used on both the Siemens and the Philips (Marconi) 4-channel scanners was co-developed by Siemens and Elscint. In this design, the 20-mm wide detector array uses eight rows of varying widths to allow simultaneous scanning of up to four 5-mm thick slices.

collimation acquisition allows retrospective reconstruction of narrower slice widths. As will be discussed later, this trade-off is complicated by the competing issues of (1) the desire for thin slices, (2) the increase in image noise for thin slices, (3) the relative radiation dose inefficiency of narrow beam collimations, and (4) data management issues (reconstruction and transfer times, archive and filming costs).

The advent of helical CT introduced an additional acquisition parameter into the CT vocabulary, *pitch*. Pitch was defined as the ratio of the table travel per x-ray tube rotation to the slice width (which was typically, but not always, equal to the beam collimation). The advent of MDCT introduced significant confusion regarding the definition of pitch, as some manufacturers used an altered definition of pitch that related the table travel per x-ray tube rotation to the width of an individual data channel. For example, using a 4-channel system ($N_{max} = 4$), a reconstructed slice width of 5 mm, a detector configuration of 4×5 mm (nominal beam collimation = 20 mm), and a table travel per rotation of 15 mm, the definition of pitch originally used with helical CT would yield 15/20 = 0.75. The manufacturer's altered definition yielded 15/5 = 3. Hence, the

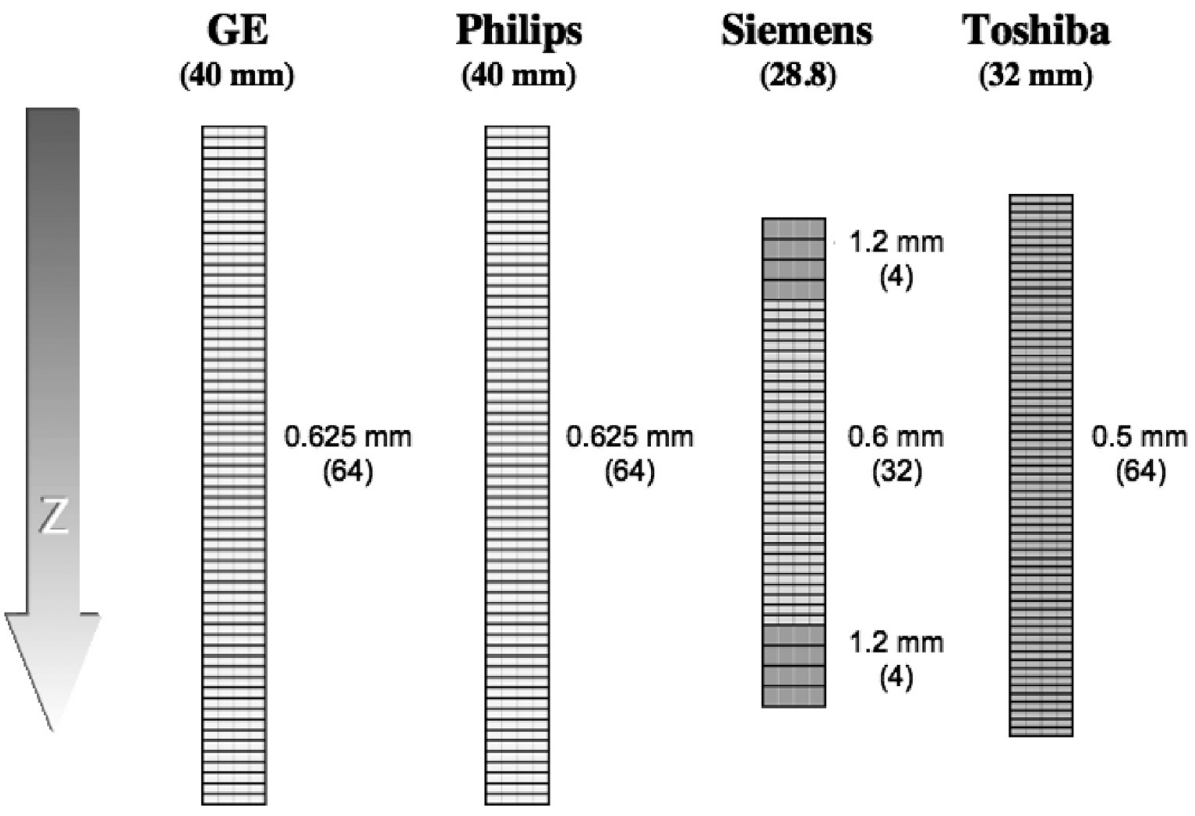

Figure 3. Diagram of the detector geometries used in 64-channel MDCT from four major manufacturers. The Siemens 64-MDCT uses 32 submillimeter detectors and a moving focal spot to achieve 64 overlapping slice measurements[17].

two definitions differed by a factor of 4 (*N*, the number of data channels used in the acquisition). As the number of data channels increased, the use of two definitions of pitch caused further confusion, as well as difficulty in comparing scan protocols and radiation dose values. Hence, the IEC reissued their CT safety standard and specifically addressed the definition of pitch, reestablishing the original definition of pitch (table travel normalized to the total beam collimation) as the only acceptable definition of pitch[3,19]. CT manufacturers altered their user interfaces accordingly for newer software releases, although older scanners with early software versions and the altered definition may still be in use. The IEC definition expresses a concept of pitch that is common to both SDCT and MDCT. From a radiation dose perspective, it is imperative to use the appropriate pitch definition (table travel per total beam collimation) because it conveys the degree of overlap of the radiation beam: a pitch of 1.0 indicates contiguous radiation beams, a pitch less than 1.0 indicates overlap of the radiation beams, and a pitch greater than 1.0 indicates gaps between the radiation beams. If this definition of MDCT pitch were not used in a radiation dose calculation, the result would be a factor of *N* too small.

As in SDCT, the tube current and the exposure time (per rotation) govern the number of x-ray photons utilized per rotation, which is given by mA • s, or simply mAs (milliamperes-second). It is important to note that just as in SDCT, mAs is indicative of *relative* output (radiation exposure) of a CT x-ray tube on a given type of CT scanner, at a given kVp. It does not indicate the absolute output (dose), as the exposure per mAs varies significantly between CT scanner manufacturers,

models, and kVp settings. Thus, 200 mAs/rotation may produce significantly different results (in dose and image quality) on different types of CT scanners and at different kVp settings. For the purpose of comparing radiation dose, mAs should be scaled to a value on each system that gives equivalent image quality (spatial resolution, contrast resolution, and noise).

Two manufacturers (Siemens and Philips) report the mAs as the average mAs along the z-axis, called either *effective* mAs or mAs/slice, where effective mAs or mAs/slice is defined as the true mAs/pitch (here they employ the IEC definition of pitch). This distinction between mAs and average mAs along the *z*-axis is very important, particularly when correcting CT dose metrics for beam overlap or gaps (pitch).

In MDCT, noise is dependent on pitch (this is not true in SDCT). Thus, as pitch is increased, MDCT scanner software may automatically increase the mA such that the image noise (and patient dose) remains relatively constant with changing pitch values[3,20]. When the *effective* mAs or mAs/slice is used, noise appears to be unaffected by pitch, since noise remains constant as pitch is varied for a constant value of effective mAs or mAs/slice. Thus, the user may be unaware that the actual mA was increased in systems that use the average mAs along the *z*-axis concept. Another manufacturer (GE) also helps the user to keep image noise constant as pitch is changed. On the GE system, as parameters such as detector configuration, pitch, or image width are changed, the mA value is automatically adjusted to the value that will keep image noise the same. In this scenario, the mA parameter field is flagged (turned orange) to alert the user of the change in the prescribed mA value.

In summary, MDCT technology offers significant improvements in the variety, quality, and speed of CT clinical applications. The technology will continue to change at a rapid pace, and radiologists, technologists, physicists and department administrators will all need to reevaluate existing practice strategies and exam protocols to successfully integrate increasingly complex MDCT scanners into their CT practice. This expected increase in utilization must be accompanied by awareness and understanding of radiation dose issues. In addition, as CT technology develops, the revision or updating of existing definitions, particularly with respect to CT dosimetry, may be required.

The purpose of this report is to provide a reference for the physics community to clarify existing definitions related to CT dosimetry, to describe methods to measure or calculate CT dose descriptors, and to discuss the issues necessary to make clinically relevant decisions regarding CT technique factors and their impact on radiation dose.

3 DEFINITIONS OF QUANTITIES FOR ASSESSING DOSE IN CT: CTDI, $CTDI_{FDA}$, $CTDI_{100}$, $CTDI_{W}$, $CTDI_{VOL}$, DLP, E

3.1 Computed Tomography Dose Index (CTDI)

The CTDI is the primary dose measurement concept in CT,

$$CTDI = \frac{1}{NT}\int_{-\infty}^{\infty} D(z)dz \ , \qquad \text{(Eqn. 1)}$$

where

$D(z)$ = the radiation dose profile along the z-axis,

N = the number of tomographic sections imaged in a single axial scan. This is equal to

the number of data channels used in a particular scan. The value of N may be less than or equal to the maximum number of data channels available on the system, and

T = the width of the tomographic section along the z-axis imaged by one data channel. In multiple-detector-row (multislice) CT scanners, several detector elements may be grouped together to form one data channel. In single-detector-row (single-slice) CT, the z-axis collimation (T) is the nominal scan width.

CTDI represents the average absorbed dose, along the z-axis, from a series of contiguous irradiations. It is measured from one *axial* CT scan (one rotation of the x-ray tube)[21–24], and is calculated by dividing the integrated absorbed dose by the nominal total beam collimation. The CTDI is always measured in the axial scan mode for a single rotation of the x-ray source, and theoretically estimates the average dose within the central region of a scan volume consisting of multiple, contiguous CT scans [Multiple Scan Average Dose (MSAD)] for the case where the scan length is sufficient for the central dose to approach its asymptotic upper limit[22,23,25]. The MSAD represents the average dose over a small interval (–I/2, I/2) about the center of the scan length ($z = 0$) for a scan interval I, but requires multiple exposures for its direct measurement. The CTDI offered a more convenient yet nominally equivalent method of estimating this value, and required only a single-scan acquisition, which in the early days of CT, saved a considerable amount of time.

3.2 $CTDI_{FDA}$

Theoretically, the equivalence of the MSAD and the CTDI requires that all contributions from the tails of the radiation dose profile be included in the CTDI dose measurement. The exact integration limits required to meet this criterion depend upon the width of the nominal radiation beam and the scattering medium. To standardize CTDI measurements (infinity is not a likely measurement parameter), the FDA introduced the integration limits of $\pm 7T$, where T represented the nominal slice width[26]. Interestingly, the original CT scanner, the EMI Mark I, was a dual-detector-row system. Hence, the nominal radiation beam width was equal to twice the nominal slice width (i.e., $N \times T$ mm). To account for this, the CTDI value must be normalized to $1/NT$:

$$CTDI_{FDA} = \frac{1}{NT} \int_{-7T}^{7T} D(z)dz. \qquad \text{(Eqn. 2)}$$

Unfortunately, the limits of integration were not similarly expressed in terms of NT, allowing for the potential underestimation of the MSAD by the CTDI. For the technology available circa 1984, the use of NT in the integration limits was deemed unnecessary at the time[27].

The scattering media for CTDI measurements were also standardized by the FDA[26]. These consist of two polymethylmethacrylate (PMMA, e.g., acrylic or Lucite™) cylinders of 14-cm length. To estimate dose values for head examinations, a diameter of 16 cm is to be used. To estimate dose values for body examination, a diameter of 32 cm is to be used. These are typically referred to, respectively, as the head and body CTDI phantoms.

3.3 $CTDI_{100}$

$CTDI_{100}$ represents the accumulated multiple scan dose at the center of a 100-mm scan and underestimates the accumulated dose for longer scan lengths. It is thus smaller than the equilibrium dose or the MSAD. The $CTDI_{100}$, like the $CTDI_{FDA}$, requires integration of the radiation

dose profile from a single axial scan over specific integration limits. In the case of $CTDI_{100}$, the integration limits are ±50 mm, which corresponds to the 100-mm length of the commercially available "pencil" ionization chamber[24,28–30].

$$CTDI_{100} = \frac{1}{NT}\int_{-50mm}^{50mm} D(z)dz \qquad \text{(Eqn. 3)}$$

The use of a single, consistent integration limit avoided the problem of dose overestimation for narrow slice widths (e.g., <3 mm)[24]. $CTDI_{100}$ is acquired using a 100-mm long, 3-cc active volume CT "pencil" ionization chamber and the two standard CTDI acrylic phantoms [head (16-cm diameter) and body (32-cm diameter)][24,26]. The measurement must be performed with a *stationary* patient table.

The pencil chamber of active length ℓ is not really measuring exposure (X), or air kerma, but rather the integral of the single rotation dose profile $D(z)$. Although the exposure (or air kerma) meter may convert the charge collected into an apparent exposure reading in roentgens (R) (or air kerma reading in milligray [mGy]), the measured value, called the "meter reading," actually represents the average exposure (or air kerma) over the chamber length ℓ. That is,

$$\text{Meter Reading} = \frac{1}{\ell}\int_{-\ell/2}^{\ell/2} X(z)dz = \frac{1}{f\cdot\ell}\int_{-\ell/2}^{\ell/2} D(z)dz\,, \qquad \text{(Eqn. 4)}$$

where f is the f-factor (exposure-to-dose conversion factor, $D = f \cdot X$).

Considering the above definition of $CTDI_{100}$ (ℓ = 100 mm), it is clear that

$$CTDI = \frac{f\left(\text{rad/R}\right)\cdot\left(\text{mm}\right)\cdot\text{meter reading}\left(\text{R}\right)}{N\cdot T\left(\text{mm}\right)}. \qquad \text{(Eqn.5)}$$

Thus

$$CTDI_{100}\left(\text{rad}\right) = \frac{\text{C}\cdot f\left(\text{rad/R}\right)\cdot 100\text{-mm}\cdot\text{meter reading}\left(\text{R}\right)}{N\cdot T\left(\text{mm}\right)}, \qquad \text{(Eqn.6)}$$

where

C = the unitless chamber calibration factor (typically near 1.0) which is required to correct the meter reading for temperature and pressure and into true exposure (if the calibration and measurement beam qualities differ sufficiently to require it).

One must use the f-factor (f) appropriate to the task at hand to convert exposure (R) to absorbed dose (rad):

- 0.78 rad/R for calculation to dose to acrylic (e.g., $CTDI_{FDA}$).
- 0.94 rad/R for tissue dose estimates.
- 0.87 rad/R for dose to air and calculation of or comparison to $CTDI_{100}$ or $CTDI_w$ (see section 3.4).
- These values correspond to the typical CT kVp value of 120 kVp, which corresponds to an effective energy of approximately 70 keV.
- For scans at other tube voltage settings, the f-factors must be chosen accordingly.

When an ion chamber measurement is given in air kerma (mGy), care must be taken to indicate which f-factor is used, if any, since the chamber reading and CTDI value are both given in units of mGy:

- 1.06 mGy/mGy for dose to tissue
- 0.90 mGy/mGy for dose to Lucite
- 1.00 mGy/mGy for dose to air.

3.4 Weighted $CDTI_W$

The CTDI varies across the field of view (FOV). For example, for body CT imaging, the CTDI is typically a factor or two higher at the surface than at the center of the FOV. The average CTDI across the FOV is estimated by the Weighted CTDI ($CTDI_w$)[19,21,31], where

$$CTDI_w = 1/3\, CTDI_{100,center} + 2/3\, CDTI_{100,edge}. \quad \text{(Eqn. 7)}$$

The values of 1/3 and 2/3 approximate the relative areas represented by the center and edge values[31]. $CTDI_w$ is a useful indicator of scanner radiation output for a specific kVp and mAs. According to IEC 60601-2-44, $CTDI_w$ must use $CTDI_{100}$ as described above and an f-factor for air (0.87 rad/R or 1.0 mGy/mGy)[19,21].

3.5 Volume $CDTI_{VOL}$

To represent dose for a specific scan protocol, which almost always involves a series of scans, it is essential to take into account any gaps or overlaps between the x-ray beams from consecutive rotations of the x-ray source. This is accomplished with use of a dose descriptor known as the Volume $CTDI_w$ ($CTDI_{vol}$), where

$$CTDI_{vol} = \frac{N \times T}{I} \times CTDI_w \quad \text{(Eqn. 8)}$$

and I = the table increment per axial scan (mm)[19].

Since pitch is defined[19] as the ratio of the table travel per rotation (I) to the total nominal beam width ($N \times T$)[3,19],

$$Pitch = \mathrm{I} \,/\, ((N \times T)), \quad \text{(Eqn. 9)}$$

Thus, Volume CTDI can be expressed as

$$CTDI_{vol} = 1 \,/\, pitch \times CTDI_w\,. \quad \text{(Eqn. 10)}$$

Whereas $CTDI_w$ represents the average absorbed radiation dose over the x and y directions at the center of the scan from a series of axial scans where the scatter tails are negligible beyond the 100-mm integration limit, $CTDI_{vol}$ represents the average absorbed radiation dose over the x, y, and z directions. It is conceptually similar to the MSAD, but is standardized with respect to the integration limits (±50 mm) and the f-factor used to convert the exposure or air kerma measurement into dose to air.

The $CTDI_{vol}$ provides a single CT dose parameter, based on a directly and easily measured quantity, which represents the average dose within the scan volume for a standardized (CTDI) phantom[19]. The SI units are milligray (mGy). $CTDI_{vol}$ is a useful indicator of the dose to a standardized phantom for a specific exam protocol, because it takes into account protocol-specific information such as pitch. Its value may be displayed prospectively on the console of newer CT scanners, although it may be mislabeled on some systems as $CTDI_w$. The IEC consensus agreement on these definitions is used on most modern scanners[19].

While $CTDI_{vol}$ *estimates* the average radiation dose within the irradiated volume for an object of similar attenuation to the CTDI phantom, it does not represent the average dose for objects of substantially different size, shape, or attenuation or when the 100-mm integration limits omit a considerable fraction of the scatter tails[32]. Further, it does not indicate the total energy deposited into the scan volume because it is independent of the length of the scan. That is, its value remains unchanged whether the scan coverage is 10 or 100 cm. It estimates the dose for a 100-mm scan length only, even though the actual volume-averaged dose will increase with scan length up to the limiting equilibrium dose value.

3.6 Dose-Length Product (DLP)

To better represent the overall energy delivered by a given scan protocol, the absorbed dose can be integrated along the scan length to compute the Dose-Length Product (DLP)[21], where

$$DLP \text{ (mGy-cm)} = CTDI_{vol} \text{ (mGy)} \times scan\ length \text{ (cm)}. \qquad \text{(Eqn. 11)}$$

The DLP reflects the total energy absorbed (and thus the potential biological effect) attributable to the complete scan acquisition. Thus, an abdomen-only CT exam might have the same $CTDI_{vol}$ as an abdomen/pelvis CT exam, but the latter exam would have a greater DLP, proportional to the greater z-extent of the scan volume.

In helical CT, data interpolation between two points must be performed for all projection angles. Thus, the images at the very beginning and end of a helical scan require data from z-axis projections beyond the defined "scan" boundaries (i.e., the beginning and end of the anatomic range over which images are desired). This increase in DLP due to the additional rotation(s) required for the helical interpolation algorithm is often referred to as "overranging." For MDCT scanners, the number of additional rotations is strongly pitch dependent, with a typical increase in irradiation length of 1.5 times the total nominal beam width.

The implications of overranging with regard to the DLP depends on the length of the imaged body region. For helical scans that are short relative to the total beam width, the dose efficiency (with regard to overranging) will decrease. For the same anatomic coverage, it is generally more dose efficient to use a single helical scan than multiple helical scans.

Table 1 illustrates the differences in $CTDI_{vol}$ and DLP for typical CT exams. The values are meant to be demonstrative only; they can vary by scanner model, vendor, and image quality requirements. Note that a change in technique (mAs/rotation) affects the $CTDI_{vol}$ (and therefore also the DLP), while a change in acquisition length (at the same technique) is only reflected by the DLP.

3.7 Limits To CTDI Methods

For body scan lengths of 250 mm or more, the accumulated dose closely approaches the limiting equilibrium dose. However, $CTDI_{100}$ underestimates the equilibrium dose CTDI (or MSAD for pitch of unity) by a factor of approximately 0.6 on the central axis and by about 0.8 on the periph-

Table 1. Illustrative values for $CTDI_{vol}$ and DLP for common CT exams for (a) 4-channel MDCT and (B) 16-channel MDCT

Table 1a: 4-channel MDCT (120 kVp)

Exam	*Beam Collimation*	*Pitch*	*mAs per Rotation*	*Scan Length (cm)*	*$CTDI_{vol}$ (mGy)*	*DLP (mGy-cm)*
Head	4 x 2.5	Axial	250	15	55.0	825
Chest	4 x 5	0.75	100	40	12.0	480
Abdomen	4 x 5	0.75	150	20	19.1	382
Abdomen ≈ & Pelvis	4 x 5	0.75	150	40	19.1	764

Table 1b: 16-channel MDCT (120 kVp)

Exam	*Beam Collimation*	*Pitch*	*mAs per Rotation*	*Scan Length (cm)*	*$CTDI_{vol}$ (mGy)*	*DLP* (mGy-cm)
Chest	16 x 1.25	0.938	150	35	13.3	466
Abdomen	16 x 1.25	0.938	212	28	18.8	526
Pelvis	16 x 1.25	0.938	212	25	18.8	470

ery[32,33]. The total energy imparted is underestimated by the DLP by a factor of about 0.7 for all scan lengths.

In order to measure the equilibrium dose, a body phantom length of almost 400 mm is required. Since a pencil chamber of this length is not practical, direct measurement of the MSAD using a conventional ion chamber[34] can be utilized. Such a method can be utilized to emulate a "virtual" pencil chamber of arbitrary length up to the available phantom length.

3.8 Effective Dose (E)

It is important to recognize that the potential biological effects from radiation depend not only on the radiation dose to a tissue or organ, but also on the biological sensitivity of the tissue or organ irradiated. A 100-mGy dose to an extremity would not have the same potential biological effect (detriment) as a 100-mGy dose to the pelvis[35]. Effective dose, *E*, is a dose descriptor that reflects this difference in biologic sensitivity[35,36]. It is a single dose parameter that reflects the risk of a non-uniform exposure in terms of an equivalent whole-body exposure. The units of effective dose are sieverts (usually millisieverts (mSv) are used in diagnostic radiology).

The concept of effective dose was designed for radiation protection of occupationally exposed personnel. It reflects radiation detriment averaged over gender and age, and its application has limitations when applied to medical populations. However, it does facilitate the comparison of biologic effect between diagnostic exams of different types[35,36.] The use of effective dose facilitates communication with patients regarding the potential harm of a medical exam that uses ionizing radiation. For example, when a patient inquires, "What dose will I receive from this exam?" an answer in the units of mGy or mGy-cm will not likely answer the more fundamental, but perhaps unspoken, question, "What is the likelihood that I will be harmed from this exam?" Characterizing the radiation dose in terms of effective dose and comparing that value to other radiation risks, for instance one year's effective dose from naturally occurring background radiation, better conveys to the patient the relative potential for harm from the medical exam. Table 2 provides typical values of effective dose for several common imaging exams (CT and non-CT), as well as the annual level of naturally occurring background radiation in the United States (≈3.0 mSv).

Table 2. Typical effective dose values for several common imaging exams (CT and non-CT)

Non-CT Typical Effective Dose Values (mSv)		*CT Typical Effective Dose Values (mSv)*	
Hand radiograph	<0.1	Head CT	1–2
Dental bitewing	<0.1	Chest CT	5–7
Chest radiograph	0.1–0.2	Abdomen CT	5–7
Mammogram	0.3–0.6	Pelvis CT	3–4
Lumbar spine radiograph	0.5–1.5	Abdomen & pelvis CT	8–14
Barium enema exam	3–6	Coronary artery calcium CT	1–3
Coronary angiogram (diagnostic)	5–10	Coronary CT angiography	5–15
Sestamibi myocardial perfusion	13–16		
Thallium myocardial perfusion	35–40		

Note:Average U.S. background radiation from naturally occurring sources ≈3.0 mSv (range 1–10 mSv)[67]

It is important to remember, however, that the effective dose describes the relative "whole-body" dose for a particular exam and scanner, but is *not* the dose for any one individual. Effective dose calculations use many assumptions, including a mathematical model of a "standard" human body that does not accurately reflect any one individual (it is androgynous and of an age representative of a radiation worker). Effective dose is best used to optimize exams and to compare risks between proposed exams. It is a broad measure of risk, and as such, should not be quoted with more than one or two significant digits.

The most direct way of estimating doses to patients undergoing CT examinations is to measure organ doses in patient-like phantoms[37]. Another way of obtaining the pattern of energy deposition in patients undergoing CT examinations is by calculation[38–40]. Computations that use Monte Carlo methods follow the paths of a large number of x-rays as they interact with a virtual phantom and estimate the probability of the dominant interaction processes (i.e., Compton scatter and photoelectric absorption). This type of calculation assumes that the patient resembles the phantom used for measurements or Monte Carlo simulation. When patients differ in size and composition, appropriate corrections might need to be used. The resultant information is the absorbed dose to a specified tissue, which may be used to predict the biological consequences to that (single) tissue. CT examinations, however, irradiate multiple tissues having different radiation sensitivities. The effective dose takes into account how much radiation is received by an individual tissue, as well as the tissue's relative radiation sensitivity[35,36].

Specific values of effective dose can be calculated using several different software packages[36], which are based on the use of data from one of two sources, the National Radiological Protection Board (NRPB) in the United Kingdom[39] or the Institute of Radiation Protection (GSF) in Germany[40]. A free Excel spreadsheet can be downloaded from *www.impactscan.org* to perform organ dose and effective dose estimates using the NRPB organ dose coefficients. Other packages are available for purchase.

To minimize controversy over differences in effective dose values that are purely the result of calculation methodology and data sources, a generic estimation method was proposed by the European Working Group for Guidelines on Quality Criteria in Computed Tomography[21]. Effective dose values calculated from the NRPB Monte Carlo organ coefficients[39] were compared to DLP values for the corresponding clinical exams to determine a set of coefficients k, where the values of k are dependent only on the region of the body being scanned (head, neck, thorax, abdomen, or pelvis) (Table 3). Using this methodology, E can be estimated from the DLP, which is reported on most CT systems:

Table 3. Normalized effective dose per dose-length product (DLP) for adults (standard physique) and pediatric patients of various ages over various body regions. Conversion factor for adult head and neck and pediatric patients assume use of the head CT dose phantom (16 cm). All other conversion factors assume use of the 32-cm diameter CT body phantom[78,79]

Region of Body	*k (mSv mGy^{-1} cm^{-1})*				
	0 year old	*1 year old*	*5 year old*	*10 year old*	*Adult*
Head and neck	0.013	0.0085	0.0057	0.0042	0.0031
Head	0.011	0.0067	0.0040	0.0032	0.0021
Neck	0.017	0.012	0.011	0.0079	0.0059
Chest	0.039	0.026	0.018	0.013	0.014
Abdomen ≈& pelvis	0.049	0.030	0.020	0.015	0.015
Trunk	0.044	0.028	0.019	0.014	0.015

$$E\,(\mathrm{mSv}) \approx k \times DLP. \qquad \text{(Eqn. 12)}$$

The values of E predicted by DLP and the values of E estimated using more rigorous calculations methods are remarkably consistent, with a maximum deviation from the mean of approximately 10% to 15%[41]. Hence, the use of DLP to estimate E appears to be a reasonably robust method for estimating effective dose. Similarly, Huda has compared effective dose, as calculated from the NRPB data[39], to estimates of energy imparted in order to develop conversion coefficients by which to later estimate effective dose from energy imparted[42].

4 OVERVIEW OF METHODS FOR DOSE REDUCTION IN CT

Recently several new approaches have focused on reducing the radiation dose required to create a CT image of appropriate diagnostic quality. Current dose reduction technical initiatives by researchers and manufacturers can be placed into one of the following general categories.

4.1 X-ray Beam Filtration

The use of an absorbent material between the x-ray tube and the patient can be used to "harden" the beam such that low-energy x-rays (which contribute disproportionately to absorbed dose) are reduced, or to "shape" the x-ray beam to deliver dose in the most appropriate spatial distribution. Previously, only head and body beam shaping (e.g., "bowtie") filters were available. Recently, manufacturers have added filters more specific to cardiac imaging or different-sized patients.

4.2 X-ray Beam Collimation

The use of a very attenuating material between the x-ray tube and the patient should be used to limit the x-ray beam to the minimal dimensions required. Such collimation occurs along the z-axis to define the radiation beam width. Additional collimation after the patient to further define the image width, whether an absorbent material or electronic, causes radiation dose to the patient to be wasted. Finally, the fan angle of the beam should be collimated to the diameter of the patient to reduce the amount of bypass that can then be scattered back towards the patient or towards personnel. Such in-plane beam collimation is typically implemented by use of an appropriate scan FOV (shaping filter).

MDCT Dose Inefficiency At Narrow Beam Collimations

MDCT systems have been observed to have a radiation dose inefficiency at narrow beam collimations[3], resulting in a higher CTDI for the narrow beam collimations required for narrow slice widths. In SDCT, CTDI is generally independent of slice width[43] (although for some SDCT systems, the CTDI can increase by as much as a factor of 2 for scan widths less than 2 mm).

The dose inefficiency in current MDCT designs is due to unused x-ray beam that strikes outside of the active area of the detector (along the *z*-direction). The *z* extent of this unused portion of the x-ray beam is approximately constant in size for the various detector configurations; thus the inefficiency caused by the unused radiation is relatively greater at narrow beam collimations. In 4-channel MDCT systems, the narrow beam dose inefficiency can be substantial, resulting in as much as a 40% to 50% dose increase for the narrow beam collimations (4×1 mm or 4×1.25 mm) relative to the widest beam collimations (4×5 mm or 4×8 mm)[3]. For submillimeter beam collimations on 4-channel MDCT systems, this dose increase can be over 100% relative to the widest beam collimations. The use of a greater number of data channels (16 or more) covering larger *z*-axis extents of the detector increases the dose efficiency of MDCT to nearly that of SDCT.

4.3 X-ray Tube Current (mAs) Modulation and Automatic Exposure Control (AEC)

It is technologically feasible for CT systems to adjust the x-ray tube current (mA) in real-time during gantry rotation in response to variations in x-ray intensity at the detector[44–47], much as fluoroscopic x-ray systems adjust exposure automatically. This capability, in various implementations, is available commercially on MDCT systems in response to wide interest from the radiology community. Some systems adapt the tube current based on changes in attenuation along the *z*-axis, others adapt to changes in attenuation as the x-ray tube travels around the patient. The ideal is to combine both approaches with an algorithm that "chooses" the correct tube current to achieve a predetermined level of image noise.

By decreasing or increasing the x-ray tube current, the radiation output of the tube is proportionately changed. Image noise is dominated by the noisiest projection (which corresponds to the most attenuating paths through the patient). Hence data acquired through body parts having less attenuation can be acquired with substantially less radiation without negatively affecting the final image noise[48–51]. This principle can be applied to modulate the mA angularly about the patient (anterior-posterior [AP] vs. lateral) as well as along the *z*-axis (neck vs. shoulders); the tube current can also be modulated within the cardiac cycle (systole vs. diastole), or with respect to sensitive organs (PA vs. AP)[44,45,52].

With regard to cardiac CT, the radiation dose for a retrospectively gated exam, where the x-ray tube is kept continuously on throughout the acquisition, can be dramatically decreased if the tube current is reduced during portions of the cardiac cycle that are not likely to be of interest for the reconstructed images. Thus, in addition to modulation of the tube current based on patient attenuation, the tube current can be modulated by the ECG signal. Since cardiac motion is least during diastole and greatest during systole, the projection data are least likely to be corrupted by motion artifact for diastolic-phase reconstructions. Accordingly, the tube current is reduced during systole. Dose reductions of approximately 50% have been reported using such a strategy[52]. The implementation of these and other dose reduction strategies is expected industrywide over the next several years, in response to the strong concern about the radiation dose from CT from both the public at large and the medical community.

In addition to technical methods of dose reduction, investigators are working to determine clinically acceptable levels of image noise for a variety of diagnostic tasks. That is, high-contrast exams

(e.g., lung, skeletal, colon, sinus) require much less dose (can tolerate higher noise levels) compared to low-contrast exams (e.g., brain, liver, and other abdominal organs). If the required noise level can be predefined, CT systems can use technical approaches to deliver the minimum dose required to achieve the specified noise level. The definition of a robust and standardized noise metric is required, however, to allow a manufacturer-independent method of prescribing the desired image quality.

4.4 Size-or Weight-based Technique Charts

Unlike traditional radiographic imaging, a CT image never looks "overexposed" in the sense of being too dark or too light; the normalized nature of CT data (i.e., CT numbers represent a fixed amount of attenuation relative to water) ensures that the image always appears properly exposed. As a consequence, CT users are not technically compelled to decrease the tube-current-time product (mAs) for small patients, which may result in excess radiation dose for these patients. It is, however, a fundamental responsibility of the CT operator to take patient size into account when selecting the parameters that affect radiation dose, the most basic of which is the mAs[12,14].

As with radiographic and fluoroscopic imaging, the operator should be provided with appropriate guidelines for mAs selection as a function of patient size. These are often referred to as technique charts. While the tube current, exposure time, and tube potential can all be altered to give the appropriate exposure to the patient, in CT users most commonly standardize the tube potential (kVp) and gantry rotation time (s) for a given clinical application. The fastest rotation time should typically be used to minimize motion burring and artifact, and the lowest kVp consistent with the patient size should be selected to maximize image contrast[47,51,53–56].

Although scan parameters can be adapted to patient size to reduce radiation dose, it is important to remember certain caveats when contemplating such adjustments. First, body regions such as the head do not vary much in size in the normal population, so modification of scan parameters may not be applicable here based on head size.

Numerous investigators have shown that the manner in which mA should be adjusted as a function of patient size should be related to the overall attenuation, or thickness, of the anatomy of interest as opposed to patient weight, which is correlated to patient girth, but not a perfect surrogate as a function of anatomic region[57–59]. The exception is for imaging of the head, where attenuation is relatively well defined by age, since the primary attenuation comes from the skull and the process of bone formation in the skull is age dependent.

Clinical evaluations of mA-adjusted images have demonstrated that radiologists do not find the same noise level acceptable in small patients as in larger patients[59]. Because of the absence of adipose tissue between organs and tissue planes, and the smaller anatomic dimensions, radiologists tend to demand lower noise images in children and small adults relative to larger patients[57–60]. For body CT imaging, typically a reduction in mA (or mAs) of a factor of 4 to 5 from adult techniques is acceptable in infants[58]. For obese patients, an increase of a factor of 2 is appropriate[58]. For head CT imaging, the mAs reduction from an adult to a newborn of approximately a factor of 2 to 2.5 is appropriate. Sample technique charts are provided in appendix A. To achieve increased exposure for obese patients, either the rotation time, or the tube potential, may also need to be increased.

4.5 Detector Geometric Efficiency

Ideally, all of the photons that pass through the patient should be used in the image formation process. However, the conversion of photon energy to electrical signal is not a 100% efficient process (although it exceeds 90% for modern scintillating detectors). New detector materials having even

higher absorption and conversion efficiencies are of course desirable, as are detector and signal processing electronics with very low inherent noise levels. Additionally, the small detector elements are divided along the detector arc and along the z axis with radiation-absorbing septa (walls). These septa also provide essential optical isolation between detector elements, but they, along with the very fine signal transmission wires, create "dead spaces" in the detector and hence waste radiation dose. As detectors continue to be divided into smaller and smaller discrete elements, the geometric efficiency of the detector systems must be maintained. One important step in reducing the dead space has been to attach and route the signal transmission wires underneath each detector element, instead of between detector elements. However, ongoing reductions in voxel size will likely be limited by the exponential increase in image noise that would accompany such changes[61].

4.6 Noise Reduction Algorithms

Data processing can be performed on the raw data (in sinogram space) or on already reconstructed images to reduce image noise. A variety of approaches are possible, all of which seek to smooth out random pixel variations (noise) while preserving fine detail and structure (signal). With a successful noise reduction scheme, an image of adequate quality can be acquired with a reduced patient dose[62].

5 CLINICAL UTILITY OF $CTDI_{VOL}$

The use of routinely displayed scan parameters such as mAs and kVp is minimally successful in predicting dose[63]. Rather than relying on parameters such as mAs, kVp, and pitch, the use of $CTDI_{vol}$ provides a single "dose metric" by which users can benchmark the prescribed output for a given exam against national averages, already having the effects of pitch, detector collimation, x-ray tube to isocenter distance, and other technical parameters all taken into account[64]. The values of $CTDI_{vol}$ displayed on the user console prior to scan initiation can be compared to published values, such as reference values provided by the American College of Radiology (ACR) and AAPM[64,65], and results of national surveys, such as the Nationwide Evaluation of X-ray Trends (NEXT) study conducted by the Center for Devices and Radiological Health (CDRH). Users prescribing doses above references values should have an appropriate justification[66].

6 APPROPRIATE USE OF CT DOSE VALUES AND RISK PARAMETERS

Effective dose estimates will vary somewhat according to the model of equipment and imaging parameters used. Typical values are given in Table 2. Effective dose estimates are only valid for prospective radiological protection purposes and should not be used for retrospective dose assessments or the detailed estimation of a specific individual's risk. Effective dose can be of some value for comparing doses from different diagnostic and therapeutic procedures and for comparing the radiation risks for different technologies, hospitals, or countries. For risk-benefit assessments for any individual, however, the absorbed dose to irradiated tissues is the more appropriate quantity.

Patient effective doses may also be compared with background radiation exposures from natural sources, which in the United States averages 3 mSv per year[67]. This allows patients and their families to put medical doses into context and better understand that radiation exposure is an everyday occurrence, not something out of the ordinary. It also obviates the need to convert doses into unfamiliar (and uncertain) radiation risk values.

The most definitive data on the ability of ionizing radiation to induce cancer is obtained from the atomic-bomb survivors cohort[8,68], albeit our knowledge of radiation risks at the relatively low radiation dose levels associated with CT scanning is subject to large uncertainties[69,70]. Current radiation risk estimates are based on a linear no threshold model, which is a topic of ongoing scientific debate[71].

Radiation risks may also be compared with those encountered in everyday life, such as the risks of dying when smoking cigarettes or the risk of dying in an automobile accident. For patients over 60 years of age, an effective dose of 17 mSv, typical of a cardiac CT angiogram, may be estimated to have a risk that is comparable to the risk of dying from lung cancer after smoking ~300 packs of cigarettes or the risk of dying in an automobile accident when driving a distance of ~12,000 miles[13,72]. Although all of these risk estimates are very crude, they do help put radiation risks into a context. More precise risk estimates require taking into account specific organ doses, age, and gender[13].

The assumption that a CT examination has a (small) radiation risk requires that all such exposures need justification and that patient doses need to be kept as low as reasonably achievable (ALARA). Examinations should not be performed when the anticipated patient benefit would be lower than the corresponding patient risk. Further, patients should not be exposed to radiation levels above those required for producing an image of diagnostic quality. A good example of minimizing patient doses is to ensure that the radiographic technique (i.e., mAs setting) is no higher than required to keep the radiographic mottle to an acceptable level[55]. Good practice also requires the use of patient-size-specific protocols and techniques that minimize dose without adversely affecting diagnostic performance[21,55,73].

In the United States there are no dose limits for patients undergoing CT examinations[35,74]. What is deemed to be an acceptable patient dose relies on the professional judgment of the physician in charge of the diagnostic procedure. To this end, it is important to ensure that imaging protocols are continually reviewed such that the choice of radiographic techniques is consistent with ALARA principles. This is best accomplished with the assistance of a diagnostic medical physicist.

7 SUMMARY

Modern CT scanners provide two dose parameters that both became available by the scanner manufacturers around 2001: the Volume CTDI ($CTDI_{vol}$) measured in mGy, and the dose-length product (DLP) measured in mGy-cm. $CTDI_{vol}$ is a measure of the average dose within the scan volume to a standardized phantom. The total amount of radiation delivered to a standardized phantom is represented by the DLP, which is the product of $CTDI_{vol}$ and the scan length. Organ doses in CT are well below the threshold for the induction of deterministic effects (e.g., erythema, epilation). Patient radiation risks in CT are therefore those related to carcinogenesis. An estimate of effective dose (E), which is related to the carcinogenic risk, may be obtained by use of E/DLP conversion factors (Table 3).

Effective doses from CT are much higher than effective doses in conventional radiography, but comparable to those associated with interventional fluoroscopic, diagnostic coronary catheterization, or nuclear medicine examinations. Although this risk from a CT examination is small, it is not zero. Hence, CT examinations should be performed only when a net patient benefit is anticipated. Further, the amount of radiation used should always be kept as low as reasonably achievable (ALARA).

This page intentionally left blank.

APPENDIX A

SAMPLES OF SIZE- OR AGE-BASED TECHNIQUE CHARTS

Head CT

1. Technique chart for Siemens Sensation 16 and 64 head and neck exams (effective mAs or mAs/slice = true mAs/pitch).
   Sequential scan mode, 24 × 1.2 mm collimation, 120 kVp

Age	Effective mAs
>10 y, adult	350
3.1 – 10 y	300
18.1 m – 3 y	260
6.1 – 18 m	235
0 – 6 m	193

2. Technique chart for General Electric CT/i (single-slice CT) head exams.
   Axial scan mode, 120 kVp

m = month; y = year

Anatomic Region	Age	Scan Width (mm) x Scan Increment (mm)	SFOV	Rotation Time (sec)	mA	$CTDI_{vol}$ (mGy)
Foramen through Petrous	0 – 6 m	3 x 3	ped	1	120	9.5
	6.1 – 18 m	3 x 3	ped	1	150	11.9
	18.1 m – 3 y	3 x 3	head	1	160	12.7
	3.1 – 10 y	3 x 3	head	1	190	15.1
	over 10 y	5 x 5	head	2	170	25.5
Top of head	0 – 6 m	7 x 7	ped	1	110	8.3
	6.1 – 18 m	7 x 7	ped	1	140	10.5
	18.1 m – 3 y	7 x 7	head	1	150	11.3
	3.1 – 10 y	7 x 7	head	1	180	13.5
	over 10 y	7 x 7	head	2	140	20.8

Body CT

1. Reference protocols for pediatric chest CT for GE LightSpeed scanners. Image width = 5 mm. Tube potential = 100 kVp. (LS = GE Light Speed; LS+ = GE Light Speed Plus; LS16 = GE Light Speed 16; LS64 = GE Light Speed VCT).

		Display Field of View Required to Display Full Patient Diameter (cm)				
Scanner	**Parameter**	**Up to 21**	**21.1 - 24**	**24.1 - 27**	**27.1 - 30**	**30.1 - 35**
LS	Tube current (mA)	90	110	150	200	180
	Rotation time (sec)	0.8	0.8	0.8	0.8	0.8
	Pitch[a]	1.5	1.5	1.5	1.5	1.5
LS+	Tube current (mA)	140	185	240	320	290
	Rotation time (sec)	0.5	0.5	0.5	0.5	0.5
	Pitch[a]	1.5	1.5	1.5	1.5	1.5
LS16	Tube current (mA)	90	115	150	200	180
	Rotation time (sec)	0.5	0.5	0.5	0.5	0.5
	Pitch[b]	0.938	0.938	0.938	0.938	0.938
LS64	Tube current (mA)	100	150	190	260	235
	Rotation time (sec)	0.4	0.4	0.4	0.4	0.4
	Pitch[c]	0.984	0.984	0.984	0.984	0.984

[a]Detector configuration: 4 x 2.5 mm, table speed: 15 mm/rotation.
[b]Detector configuration: 16 x 1.25 mm, table speed: 18.75 mm/rotation.
[c]Detector configuration: 64 x 0.625 mm, table speed: 39.38 mm/rotation.

Body CT (cont.)

2. Relative technique chart for abdominal and pelvis CT in children and adults. Applies to any CT system or kVp, since all mAs values are normalized to the site's reference protocol (shown in **bold**, relative mAs = 1). The lateral patient width at the level of the liver is measured from the CT radiograph (Scout, Topogram, etc.).

Abdomen & Pelvis CT Technique Chart for Children (<22.1 cm)

Lateral Patient Width (cm) at Level of the Liver	mAs (relative to standard pediatric protocol)
up to 14	0.55
14.1 – 18	0.75
18.1 – 22	**1.00**

Abdomen & Pelvis CT Technique Chart for Adults (>22 cm)

Lateral Patient Width (cm) at Level of the Liver	mAs (relative to standard adult protocol)
22.1 – 26	0.4
26.1 – 30	0.5
30.1 – 35	0.7
35.1 – 40	**1.0**
40.1 – 45	1.4
45.1 – 50	2.0

APPENDIX B

REVIEW OF AUTOMATIC EXPOSURE CONTROL (AEC) SYSTEMS USED ON COMMERCIAL CT SYSTEMS

The following section on Automatic Exposure Control systems is a condensed version of a report by the ImPACT group, which can be freely downloaded from www.impactscan.org/reports/Report05016.htm ("MHRA Report 05016 - CT scanner automatic exposure control systems", Nicholas Keat, HMSO 2005. ISBN 1-84182-947 -1).*Imaging Performance Assessment of CT Scanners, www.impactscan.org.*

Background

All CT scanners have a range of pre-programmed protocols for different examination types, with set values for tube potential, tube current, rotation time, slice width, etc. These will generally be set up for an "average" sized patient. The operator of the scanner can vary these parameters on a patient-by-patient basis, usually through modification of the tube current or rotation time in order to change the mAs (tube current – time product). For example, a large patient will need a higher than average mAs to counteract the effect of increased attenuation and the resultant increase in image noise. Similarly, CT scans of a small adult, or child, will demonstrate adequate image quality at a lower mAs than that required for a "typical" patient. The degree to which the parameters are altered depends on the institution, but in many cases it is left to the judgment of the operator. A more repeatable way of adjusting tube current for different-sized patients is to relate it to some measured characteristic of the patient such as height and/or weight, body mass index, or lateral width[58,75].

Over recent years, the introduction of AEC systems for CT has allowed the sort of adjustment described above to be performed automatically on a patient-by-patient basis. In addition, the AEC systems can adjust the tube current within a patient as the patient's attenuation varies. This finer degree of tube current control was not possible with manual tube current adjustments. While AEC systems have a number of potential advantages, including consistency of image quality and better control of patient radiation dose, the operator is responsible to use these systems correctly, and this requires education about the capabilities of particular AEC systems and the methods for controlling their operation.

Automatic control of tube current

The general aim of an AEC system for CT is to significantly reduce or eliminate variations in image quality between different images. This also reduces the variation in radiation doses to different-sized patient cross sections. On present systems, this is achieved through the control of the x-ray tube current to achieve the required level of image noise.

This can work at three levels:

Patient size AEC. The AEC system adjusts the tube current based upon the overall size of the patient. The same mA is used for an entire examination or scan series. The aim is to reduce the variation in image quality from patient to patient and prevent unnecessarily high doses to small patients.

Z-axis AEC. The tube current is adjusted for each rotation of the x-ray tube, taking into account the variation in attenuation along the patient's *z*-axis (from head to toe).

Rotational AEC. The tube current is decreased and increased rapidly (modulated) during the course of each rotation to compensate for differences in attenuation between lateral (left-right) and AP (anterior-posterior) projections. In general, lateral projections are more attenuating than AP, particularly in asymmetric regions of the body such as the shoulders or pelvis[44,45].

Current implementations tend to combine two or all three of these types of tube current adjustment[51]. Image noise is affected by rotational AEC in a different manner relative to patient and *z*-axis AEC. Rotational AEC attempts to reduce the variation in uncertainty of attenuation measurements by increasing the tube current through the most attenuating projection angles, and reducing the mA where the attenuation is lowest. The effect on the image is to even out variations in image noise across the field of view. This can reduce the severity of photon starvation artifacts through asymmetric body regions.

Another application of CT AEC is in cardiac scanning, where the tube current is modulated based upon the patient's ECG signal. Cardiac images are normally reconstructed during diastole, where myocardial movement is lowest. The x-ray tube current can therefore be reduced during systole since images are not typically reconstructed at this point in the cardiac cycle. Dose reductions up to 50% have been reported[52].

Whilst most scanner manufacturers aim to keep image quality constant from patient to patient, and from slice to slice within one patient, this is not always felt to be desirable. There is evidence that the level of image quality required to make adequate diagnoses varies with the size of patient[58,59,75,76]. For small patients, particularly children, radiologists typically require less noisy images than for larger patients and adults. For this reason, one manufacturer offers various "strengths" of tube current adaptation, all of which will compensate for patient size but not as much as would be needed to keep image quality constant for different sized patients[51].

Scanner requirements

CT AECs place special demands upon scanner hardware and require additional software in order to operate. The hardware needs to be able to rapidly and predictably vary the x-ray output, which impacts upon the generator and the x-ray tube.

Software is required to assess the size of the patient in order that an appropriate tube current can be set. CT radiographs (scout, scanogram, or topogram views) are the main way that AEC systems assess the attenuation of the patient along their length. This information can be used as the basis for patient and *z*-axis AEC and can supply some information for rotational AEC. Rotational AEC can also use feedback from the attenuation measurements made during the course of the CT scan. Changes in the patient profile generally occur gradually along the *z*-axis, so the shape of the attenuation profile at each angle during each rotation can be used to control the tube current during the next rotation.

AEC software must also allow the user to control the exposure and image quality. Present methods are as follows:

Standard deviation–based AEC control. Using this method, the user controls the AEC by specifying image quality in terms of the resultant standard deviation (SD) of pixel values. Setting a high SD value gives a noisy image; low SD settings give low-noise

images. The scanner aims to set the tube current that is required to achieve the requested standard deviation on an image-by-image basis.

Reference mAs AEC control. This method of AEC control uses the familiar concept of setting an mA (or mAs) value for a given protocol; in this case a "reference" mAs is used. This is the value that would be used for an average-sized patient. The AEC system assesses the size of the patient cross section being scanned and adjusts the tube current relative to the reference value.

Reference image AEC control. The third approach that is currently used for controlling AEC systems is to use a "reference image" that has previously been scanned and judged to be of appropriate quality for a particular clinical task. The scanner attempts to adjust the tube current to match the noise in the reference image.

Practical use of AEC systems

AEC systems have been primarily developed as part of manufacturers' dose reduction or dose management programs. While the use of AEC should generally lead to reduced patient doses, it is also possible to operate an AEC system in a way that results in higher patient doses than would occur with a standard fixed mA system. AEC systems do not reduce patient dose per se, but enable scan protocols to be prescribed using measures related to image quality. If the required image quality is specified appropriately by the user, and suited to the clinical task, then a reduction in patient dose can be expected for most patients[48,49,51,77].

Although setting the x-ray tube current is only part of the wider task of protocol optimization, the use of AEC takes the guesswork out of adjusting mA. The key to ensuring the image quality is set correctly is to use an appropriate image noise level, reference mAs or reference image in the AEC setup. This is not a straightforward process. One method of approaching this goal is to focus image quality assessment upon depiction of clinically relevant pathology, such as is outlined in the *European Guidelines on Quality Criteria for Computed Tomography*[21]. Another method that has potential promise for the future is the use of software tools that allow users to simulate the effect of increasing image noise in a clinical image.

One of the challenges facing users involved in modifying clinical scan protocols is gaining knowledge of the way that the various scan and reconstruction parameters affect image quality and patient dose. Although the use of CT AEC is generally quite straightforward, there are significant differences from one vendor's system to another. In particular, the dependence of the AEC tube current setting depends upon different scan parameters, such as tube voltage, image thickness and reconstruction kernel. There is no obvious correct or incorrect way for vendors to program the response of their AEC, but it is critically important that users are aware of the behavior of their system and the effect that varying scan and reconstruction parameters has upon the AEC.

The best method to check the effect of the use of an AEC system upon patient doses is to monitor the scanner's own dose indicators. All modern scanners now display routinely the $CTDI_{vol}$ and DLP for each examination. By monitoring these parameters before and after the introduction of an AEC, its effect upon radiation dose for different exam types can be assessed. AEC exposure levels can be modified if necessary with reference to these data, although one should also account for the effect of changing any other parameters, such as beam collimation or kV.

REFERENCES

1. Liang Y, Kruger RA. (1996) "Dual-slice spiral versus single-slice spiral scanning: comparison of the physical performance of two computed tomography scanners." *Med Phys* 23:205–220.
2. Hu H. (1999) "Multi-slice helical CT: Scan and reconstruction." *Med Phys* 26:5–18.
3. McCollough CH, Zink FE. (1999). "Performance evaluation of a multi-slice CT system." *Med Phys* 26:2223–2230.
4. Mori S, Endo M, Tsunoo T, Kandatsu S, Tanada S, Aradate H, Saito Y, Miyazaki H, Satoh K, Matsushito S, Kusakabe M. (2004) "Physical performance evaluation of a 256-slice CT-scanner for four-dimensional imaging." *Med Phys* 31:1348–1356.
5. Brenner DJ, Elliston CD, Hall EJ, Berdon WE. (2001) "Estimated risks of radiation-induced fatal cancer from pediatric CT." *AJR Am J Radiol* 176:289–296.
6. Donnelly LF, Emery KH, Brody AS, Laor T, Gylys-Morin VM, Anton CG, Thomas SR, Frush DP. (2001) "Minimizing radiation dose for pediatric body applications of single-detector helical CT: Strategies at a large children's hospital." *AJR Am J Radiol* 176:303–306.
7. Sternberg S. (CT scans in children linked to cancer." *USA Today*, June 19, 2001.
8. Pierce DA, Preston DL. (2000) "Radiation-related cancer risks at low dose among atomic bomb survivors." *Radiat Res* 154:178–186.
9. Haaga JR. (2001) "Radiation dose management: weighing risk versus benefit." *AJR Am J Roentgenol* 177:289–291.
10. Nickoloff EL, Alderson PO. (2001) "Radiation exposures to patients from CT: Reality, public perception, and policy." *AJR Am J Roentgenol* 177:285–287.
11. Brenner DJ. (2002) "Estimating cancer risks from pediatric CT: Going from the qualitative to the quantitative." *Pediatr Radiol* 32:228–223; discussion 242–244.
12. FDA. (2002) "FDA public health notification: reducing radiation risk from computed tomography for pediatric and small adult patients." *Pediatr Radiol* 32:314–316.
13. Einstein AJ, Henzlova MJ, Rajagopalan S. (2007) "Estimating risk of cancer associated with radiation exposure from 64-slice computed tomography coronary angiography." *JAMA* 298:317–323.
14. Linton OW, Mettler FA, Jr. (2003) "National conference on dose reduction in CT, with an emphasis on pediatric patients." *AJR Am J Roentgenol* 181:321–329.
15. Mettler FA, Jr., Wiest PW, Locken JA, Kelsey CA. (2000) "CT scanning: Patterns of use and dose." *J Radiol Prot* 20:353–359.
16. IMV. Benchmark Report CT. In: Young L, ed. Des Plaines, IL: IMV Medical Information Division, Inc., 2006. www.IMVinfo.com.
17. Flohr TG, Stierstorfer K, Ulzheimer S, Bruder H, Primak AN, McCollough CH. (2005) "Image reconstruction and image quality evaluation for a 64-slice CT scanner with z-flying focal spot." *Med Phys* 32:2536–2547.
18. Flohr TG, Schaller S, Stierstorfer K, Bruder H, Ohnesorge BM, Schoepf UJ. (2005) "Multi-detector row CT systems and image-reconstruction techniques." *Radiology* 235:756–773.
19. International Electrotechnical Commission (IEC). Medical Electrical Equipment. Part 2-44: Particular requirements for the safety of x-ray equipment for computed tomography. IEC publication No. 60601-2-44. Ed. 2.1: International Electrotechnical Commission (IEC) Central Office: Geneva, Switzerland, 2002.
20. Mahesh M, Scatarige JC, Cooper J, Fishman EK. (2001) "Dose and pitch relationship for a particular multislice CT scanner." *AJR Am J Roentgenol* 177:1273–1275.
21. Jessen KA, Panzer W, Shrimpton PC, et al. EUR 16262: European Guidelines on Quality Criteria for Computed Tomography. Luxembourg: Office for Official Publications of the European Communities, 2000.
22. Nagel HD. Radiation Exposure in Computed Tomography. The European Coordination Committee of the Radiological and Electromedical Healthcare IT Industry (COCIR), Frankfurt, 2000.
23. Shope TB, Gagne RM, Johnson GC. (1981) "A method for describing the doses delivered by transmission x-ray computed tomography." *Med Phys* 8:488–495.
24. American Association of Physicists in Medicine (AAPM) Report 31. Standardized Methods for Measuring Diagnostic X-ray Exposures. New York: AAPM, 1990.
25. McCrohan JL, Patterson JF, Gagne RM, Goldstein HA. (1987) "Average radiation doses in a standard head examination for 250 CT systems." *Radiology* 163:263–268.

26. U. S. Food and Drug Administration (FDA). Diagnostic X-Ray Systems and Their Major Components. *Code of Federal Regulations*. 21 *CFR* 1020.33, 1984.
27. Dixon RL. (2006) "Restructuring CT dosimetry--a realistic strategy for the future Requiem for the pencil chamber." *Med Phys* 33:3973–3976.
28. Jucius RA, Kambic GX. (1980) "Measurements of computed tomography x-ray fields utilizing the partial volume effect." *Med Phys* 7:379–382.
29. American Association of Physicists in Medicine (AAPM) Report 39. Specification and Acceptance Testing of Computed Tomography Scanners. New York: AAPM, 1993.
30. McNitt-Gray MF. (2002) "AAPM/RSNA physics tutorial for residents: Topics in CT. Radiation dose in CT." *Radiographics* 22:1541–1553.
31. Leitz W, Axelsson B, Szendro G. (1995) "Computed tomography dose assessment: A practical approach." *Radiat Prot Dosim* 57:377–380.
32. Boone JM. (2007) "The trouble with CTDI 100." *Med Phys* 34:1364–1371.
33. Mori S, Endo M, Nishizawa K, Tsunoo T, Aoyama T, Fujiwara H, Murase K. (2005) "Enlarged longitudinal dose profiles in cone-beam CT and the need for modified dosimetry." *Med Phys* 32:1061–1069.
34. Dixon RL. (2003) "A new look at CT dose measurement: Beyond CTDI." *Med Phys* 30:1272–1280.
35. International Commission on Radiological Protection (ICRP) Report 60. 1990 Recommendations of the International Commission on Radiological Protection. *Annals of the ICRP* 21:1/3, 1991.
36. McCollough CH, Schueler BA. (2000) "Calculation of effective dose." *Med Phys* 27:828–837.
37. Huda W, Sandison GA. (1986) "The use of the effective dose equivalent, HE, as a risk parameter in computed tomography." *Br J Radiol* 59:1236–1238.
38. Jarry G, DeMarco JJ, Beifuss U, Cagnon CH, McNitt-Gray MF. (2003) "A Monte Carlo-based method to estimate radiation dose from spiral CT: From phantom testing to patient-specific models." *Phys Med Biol* 48:2645–2663.
39. Jones DG, Shrimpton PC. Survey of CT Practice in the UK. Part 3: Normalised Organ Doses Calculated Using Monte Carlo techniques. Oxon: National Radiological Protection Board, 1991.
40. Zankl M, Panzer W, Drexler G. The Calculation of Dose from External Photon Exposures Using Reference Human Phantoms and Monte Carlo Methods. Part VI: Organ Doses from Computed Tomographic Examinations. Neuherberg, Germany: GSF - Forschungszentrum fur Umwelt und Gesundtheit, Institut fur Strahlenschutz, 1991.
41. McCollough CH. (2003) "Patient dose in cardiac computed tomography." *Herz* 28:1-6.
42. Huda W, Atherton JV, Ware DE, Cumming WA. (1997) "An approach for the estimation of effective radiation dose at CT in pediatric patients." *Radiology* 203:417–422.
43. McNitt-Gray MF, Cagnon C, Solberg TD, Chetty I. (1999) "Radiation dose from spiral CT: The relative effects of collimation and pitch." *Med Phys* 26:409–414.
44. Gies M, Kalender WA, Wolf H, Suess C, Madsen M. (1999) "Dose reduction in CT by anatomically adapted tube current modulation: Simulation studies." *Med Phys* 26:2235–2247.
45. Kalender WA, Wolf H, Suess C. (1999) "Dose reduction in CT by anatomically adapted tube current modulation: Phantom measurements." *Med Phys* 26:2248–2253.
46. Haaga JR, Miraldi F, MacIntyre W, LiPuma JP, Bryan PJ, Wiesen E. (1981) "The effect of mAs variation upon computed tomography image quality as evaluated by in vivo and in vitro studies." *Radiology* 138:449–454.
47. McCollough CH. (2005) "Automatic exposure control in CT: Are we done yet?" *Radiology* 237:755–756.
48. Graser A, Wintersperger BJ, Suess C, Reiser MF, Becker CR. (2006) "Dose reduction and image quality in MDCT colonography using tube current modulation." *AJR Am J Roentgenol* 187:695–701.
49. Greess H, Wolf H, Baum U, Lell M, Pirkl M, Kalender W, Bautz WA. (2000) "Dose reduction in computed tomography by attenuation-based, on-line modulation of tube current: Evaluation of six anatomical regions." *Eur Radiol* 10:391–394.
50. Mulkens TH, Bellinck P, Baeyaert M, Ahysen D, Van Dijck X, Mussen E, Venstermans C, Termote JL. (2005) "Use of an automatic exposure control mechanism for dose optimization in multi-detector row CT examinations: Clinical evaluation." *Radiology* 237:213–223.
51. McCollough CH, Bruesewitz MR, Kofler JM, Jr. (2006) "CT dose reduction and dose management tools: Overview of available options." *Radiographics* 26:503–512.

52. Jakobs TF, Becker CR, Ohnesorge B, Flohr T, Suess C, Schoepf VJ, Reiser M. (2002) "Multislice helical CT of the heart with retrospective ECG gating: Reduction of radiation exposure by ECG-controlled tube current modulation." *Eur Radiol* 12:1081–1086.
53. Funama Y, Awai K, Nakayama Y, Kakei K, Nagasue N, Shimamura M, Sato N, Sultana S, Morishita S, Yamashita Y. (2005) "Radiation dose reduction without degradation of low-contrast detectability at abdominal multisection CT with a low-tube voltage technique: phantom study." *Radiology* 237:905–910.
54. Nakayama Y, Awai K, Funama Y, Hatemura M, Imuta M, Nakaura T, Ryu Da, Morishita S, Sultana S, Sato N, Yamashita Y. (1005) "Abdominal CT with low tube voltage: Preliminary observations about radiation dose, contrast enhancement, image quality, and noise." *Radiology* 237:945–951.
55. Huda W, Ravenel JG, Scalzetti EM. (2002) "How do radiographic techniques affect image quality and patient doses in CT?" *Semin Ultrasound CT MR* 23:411–422.
56. Siegel MJ, Schmidt B, Bradley D, Suess C, Hildebolt C. (2004) "Radiation dose and image quality in pediatric CT: effect of technical factors and phantom size and shape." *Radiology* 233:515–522.
57. Boone JM, Geraghty EM, Seibert JA, Wootton-Gorges SL.(2003) "Dose reduction in pediatric CT: A rational approach." *Radiology* 228:352–360.
58. McCollough CH, Zink FE, Kofler J, Matsumoto JS, Thomas KB, Hoffman AD. (2002) "Dose optimization in CT: Creation, implementation and clinical acceptance of size-based technique charts." *Radiology* 225(P):591.
59. Wilting JE, Zwartkruis A, van Leeuwen MS, Timmer J, Kamphuis AG, Feldberg M. (2001) "A rational approach to dose reduction in CT: Individualized scan protocols." *Eur Radiol* 11:2627–2632.
60. Kalra MK, Maher MM, Toth TL, Schmidt B, Westerman BL, Morgan HT, Saini S. (2004) "Techniques and applications of automatic tube current modulation for CT." *Radiology* 233:649–657.
61. Fuchs T, Kalender W. (2003) "On the correlation of pixel noise, spatial resolution and dose in computed tomography: Theoretical prediction and verification by simulation and measurement." *Physica Medica* 19:153–164.
62. Raupach R, Bruder H, Stierstorfer K, Suess C, Flohr T. A Novel Approach for Efficient Edge Preserving Noise Reduction in CT Volume Data (abstract). Radiological Society of North America Annual Meeting Program. Chicago, IL, 2005.
63. Herlihy V, McCollough CH, Branham TA, Bush KM, Zeman RK. Use of Clinical CT Scan Parameters to Predict Patient Dose versus Measured CT Dose Index (CTDIw): An Analysis of the American College of Radiology (ACR) CT Accreditation Database. Radiological Society of North America 2006. Chicago, IL, 2006.
64. McCollough CH. (2006) "It is time to retire the computed tomography dose index (CTDI) for CT quality assurance and dose optimization. Against the proposition." *Med Phys* 33:1190–1191.
65. Gray JE, Archer BR, Butler PF, Hobbs BB, Mettler FA, Jr., Pizzutiello RJ, Jr., Schueler BA, Strauss KJ, Suleiman OH, Yaffe MJ. (2005) "Reference values for diagnostic radiology: Application and impact." *Radiology* 235:354–358.
66. Hart D, Hillier MC, Wall BF, Shrimpton PC, Bungay D. Doses to Patients from Medical X-ray Examinations in the UK: 1995 review. National Radiological Protection Board Publication NRPB-R289. Chilton, Didcot, Oxon, England: NRPB, 1996.
67. National Council on Radiation Protection and Measurements. Ionizing Radiation Exposure of the Population of the United States. Report No. 93. Bethesda, MD: NCRP, 1987.
68. Preston DL, Shimizu Y, Pierce DA, Suyama A, Mabuchi K. (2003) "Studies of mortality of atomic bomb survivors. Report 13: Solid cancer and noncancer disease mortality: 1950–1997." *Radiat Res* 160:381–407.
69. Brenner DJ, Doll R, Goodhead DT, Hall EJ, Land CE, Little JB, Lubin JH, Preston DL, Preston RJ, Puskin JS, et al. (2003) "Cancer risks attributable to low doses of ionizing radiation: Assessing what we really know." *Proc Natl Acad Sci USA* 100:13761–13766.
70. National Council on Radiation Protection and Measurements. Uncertainties in Fatal Cancer Risk Estimates Used in Radiation Protection. Report No. 126. Bethesda, MD: NCRP, 1997.
71. National Council on Radiation Protection and Measurements. Evaluation of the Linear-Nonthreshold Dose-Response Model for Ionizing Radiation. Report No. 136. Bethesda, MD: NCRP, 2001.
72. Hall EJ. *Radiobiology for the Radiologist*. Philadelphia, PA: Lippincott Williams & Wilkins, 1994.
73. Kalra MK, Maher MM, Toth TL, Hamberg LM, Blake MA, Shepard JA, Saini S. (2004) "Strategies for CT radiation dose optimization." *Radiology* 230:619–628.

74. International Commission on Radiological Protection. (2000) "Managing patient dose in computed tomography. A report of the International Commission on Radiological Protection." *Ann ICRP* 30:7–45.
75. Boone JM. (2005) "What parameters are most accurate in predicting appropriate technique factors for CT scanning?" *Radiology* 236:377–378.
76. Kalra MK, Maher MM, Kamath RS, Horiuchi T, Toth TL, Halpern EF, Saini S. (2004) "Sixteen-detector row CT of abdomen and pelvis: Study for optimization of z-axis modulation technique performed in 153 patients." *Radiology* 233:241–249.
77. Mulkens TH, Bellinck P, Baeyaert M, Ghysen D, Van Dijck X, Mussen E, Venstermans C, Termote JL. (2005) "Use of an automatic exposure control mechanism for dose optimization in multi-detector row CT examinations: Clinical evaluation." *Radiology* 237:213–223.
78. Bongartz G, Golding S, Jurik A, Leonardi M, van Meerten EvP, Geleijns J, Jessen KA, Panzer W, Shrimpton PC, Tosi G. European Guidelines for Multislice Computed Tomography. European Commission 2004.
79. Shrimpton PC, Hillier MC, Lewis MA, Dunn M. (2006) "National survey of doses from CT in the UK: 2003." *Br J Radiol* 79:968–980.